Contents lists available at ScienceDirect

International Journal of Pharmaceutics

Functional ibuprofen-loaded cationic nanoemulsion: Development and optimization for dry eye disease treatment

Bisera Jurišić Dukovski[a], Marina Juretić[b], Danka Bračko[b], Danijela Randjelović[c], Snežana Savić[d], Mario Crespo Moral[e], Yolanda Diebold[e,f], Jelena Filipović-Grčić[a], Ivan Pepić[a], Jasmina Lovrić[a,*]

[a] University of Zagreb, Faculty of Pharmacy and Biochemistry, Department of Pharmaceutical Technology, Zagreb, Croatia
[b] R&D, PLIVA Croatia Ltd, TEVA Group Member, Zagreb, Croatia
[c] University of Belgrade, Institute of Chemistry, Technology and Metallurgy, Department of Microelectronic Technologies, Belgrade, Serbia
[d] University of Belgrade, Faculty of Pharmacy, Department of Pharmaceutical Technology and Cosmetology, Belgrade, Serbia
[e] University of Valladolid, Institute of Applied Ophthalmo-Biology (IOBA), Valladolid, Spain
[f] Biomedical Research Networking Center on Bioengineering, Biomaterials and Nanomedicine (CIBER-BBN), Valladolid, Spain

ARTICLE INFO

ABSTRACT

Inflammation plays a key role in dry eye disease (DED) affecting millions of people worldwide. Non-steroidal anti-inflammatory drugs (NSAIDs) can be used topically to act on the inflammatory component of DED, but their limited aqueous solubility raises formulation issues. The aim of this study was development and optimization of functional cationic nanoemulsions (NEs) for DED treatment, as a formulation approach to circumvent solubility problems, prolong drug residence at the ocular surface and stabilize the tear film. Ibuprofen was employed as the model NSAID, chitosan as the cationic agent, and lecithin as the anionic surfactant enabling chitosan incorporation. Moreover, lecithin is a mixture of phospholipids including phosphatidylcholine and phosphatidylethanolamine, two constituents of the natural tear film important for its stability. NEs were characterized in terms of droplet size, polydispersity index, zeta-potential, pH, viscosity, osmolarity, surface tension, entrapment efficiency, stability, sterilizability and *in vitro* release. NEs mucoadhesive properties were tested rheologically after mixing with mucin dispersion. Biocompatibility was assessed employing 3D HCE-T cell-based model and *ex vivo* model using porcine corneas. The results of our study pointed out the NE formulation with 0.05% (*w/w*) chitosan as the lead formulation with physicochemical properties adequate for ophthalmic application, mucoadhesive character and excellent biocompatibility.

1. Introduction

A stable preocular tear film is a hallmark of ocular health, as it protects and moisturizes cornea and forms the primary refracting surface for light entering the visual system (Willcox et al., 2017). A two layered model of the tear film has been proposed, consisting of: (i) a mucoaqueous gel layer making up the bulk of the tear thickness and interacting directly with the epithelium, and (ii) an overlying very thin lipid layer, at least partly integrated with the mucoaqueous gel. Dry eye disease (DED), a multifactorial disease of the ocular surface, is characterized by a loss of homeostasis of the tear film (Craig et al., 2017).

The loss of homeostasis involves a quantitative or qualitative deficiency of tears that typically induces tear film instability, wetting defects and hyperosmolar stress, increased friction and chronic mechanical irritation at the ocular surface (Bron et al., 2017). This initiates a chain of inflammatory events and further ocular surface damage.

Currently, the main therapeutic options for DED are tear replacement and topical anti-inflammatory therapy (Jones et al., 2017). A topical ophthalmic formulation with or without an active pharmaceutical ingredient (API) is delivered directly on the ocular surface and excipients used in the formulation play an essential role in addressing quantitative or qualitative deficiency of tears. There are numerous over-

the-counter products (artificial tears) aiming to replace and/or supplement the tear film. The most abundant component in these lubricant eye drops is the aqueous base with a variety of viscosity enhancing agents incorporated to improve lubrication and prolong the retention time on the ocular surface. More recently, a variety of lipids (e.g. mineral oils and phospholipids) have been incorporated in ocular lubricant formulations to help restoration of the tear film lipid layer (Benelli, 2011). APIs aiming at decreasing inflammation at the ocular surface include glucocorticoids, non-glucocorticoid immunomodulators (i.e. cyclosporine A (CsA) and tacrolimus), non-steroidal anti-inflammatory drugs (NSAIDs) and antibiotics (Jones et al., 2017).

Oil-in-water (O/W) nanoemulsions (NEs), ultrafine dispersions stabilized by an amphiphilic surfactant (Singh et al., 2017), hold great potential for effective treatment of DED (Jones et al., 2017; Lallemand et al., 2017). According to current understanding, mixing of a NE with the tear film compromises NE stability, the oil nanodroplets break down with time, the oil merges with the lipid layer of the tear film, and the surfactant components associate with the mucus layer (Gan et al., 2013; Walenga et al., 2019). Supplementation of a deficient tear film lipid layer (TFLL) with appropriate lipid components by merging with oil droplets possibly induces tear film stabilization. Furthermore, NEs effectively deliver APIs with limited aqueous solubility into the corneal segment giving delayed and sustained release (Lalu et al., 2017). This can be ascribed to oil nanodroplets that act as an API reservoir before and after merging with TFLL. As the majority of anti-inflammatory APIs have limited aqueous solubility, API-loaded NE can assure dry eye symptom relief due to tear film stabilization as well as anti-inflammation effects breaking the vicious circle of DED.

Over the past two decades NEs have been seriously investigated as a strategy to enhance the eye-related bioavailability of CsA following topical ocular instillation (Lallemand et al., 2017). These efforts led to the commercialization of three NE-based ophthalmic products for treatment of DED. Restasis® (Allergan) is a preservative-free anionic O/W NE of CsA-loaded castor oil, emulsified and stabilized by polysorbate 80 and carbomer copolymer, approved by the U.S. Food and Drug Administration (FDA). Lacrinmune® (Bausch & Lomb, approved in Argentina) has a composition similar to that of Restasis®, except for the addition of sodium hyaluronate which increases formulation viscosity with the aim to prolong the residence time at the ocular surface. Ikervis® (Santen) is a cationic NE of medium-chain triglycerides emulsified and stabilized using tyloxapol, poloxamer 188 and cetalkonium chloride, approved by the European Medicines Agency (EMA). In this formulation quaternary ammonium cetalkonium chloride, an alkyl derivative of benzalkonium chloride, does not have a preservative role but it renders the oil nanodroplets positively charged. The presence of positive charge on the nanodroplet surface enables their electrostatic interaction with negatively charged ocular surface mucins, improving formulation precorneal residence (Daull et al., 2014). It is therefore assumed that the residence time of CsA in Ikervis® is longer than that in Restasis® (Lallemand et al., 2012), which, accompanied with higher dosage strength, could very likely explain the difference in dosing regimen between once-a-day Ikervis® versus twice-a-day Restasis® (Lallemand et al., 2017).

CsA is used in the treatment of more severe cases of DED; it has to be used for extended periods of time and its onset of action is postponed. Topical glucocorticoid or NSAID short-term pre-treatment could provide faster sign and symptom relief than topical CsA alone in severe DED (Jones et al., 2017). Moreover, topical glucocorticoids or NSAIDs have a potential for effective treatment of mild-to-moderate DED. Development of formulations with prolonged residence at the ocular surface would enable reduction of the required dose of glucocorticoids and NSAIDs providing better benefit-risk balance of future ophthalmic drug products (Subrizi et al., 2019). Therefore, further investigations are needed to explore the potential of glucocorticoids or NSAIDs in a pulse-dose form to break the vicious circle of DED, to develop effective formulations and to clarify the appropriate dosing schedules.

In this study, we propose the development of a functional cationic ophthalmic NE loaded with a NSAID aiming to relieve dryness, stabilize the tear film and act on the inflammatory component in mild-to-moderate DED patients. Special attention was paid to the selection of excipients in order to achieve optimal balance between formulation properties (droplet size and size distribution, zeta-potential, osmolarity, viscosity, surface tension and stability) and formulation effect on the ocular surface (mucoadhesion, tear film and corneal epithelium biocompatibility). The mucoadhesive biopolymer chitosan was chosen as a carrier of positive charge and was incorporated in NE using its interaction with the anionic surfactant lecithin. Lecithin is a natural lipid mixture of phospholipids including phosphatidylcholine and phosphatidylethanolamine, two phospholipids that are commonly found in tears (Dean and Glasgow, 2012; Jones et al., 2017; Saville et al., 2011). Kolliphor® EL, a non-ionic surfactant commonly used in ophthalmic products, was used as the second (more hydrophilic) surfactant to optimize the NE droplet size and stability (Trotta et al., 2002). Ibuprofen was used as the model NSAID of highly lipophilic nature. The formulation biocompatibility assessment employing appropriate *in vitro* and *ex vivo* models has been included in this early phase of formulation development.

2. Materials and methods

2.1. Materials

Ibuprofen (Hubei Biocause Phamaceutical Co., Ltd., Jingmen, China) was kindly donated by Pliva (Zagreb, Croatia). For NE preparation the following substances were used: Miglyol® 812 (Kemig, Zagreb, Croatia), lecithin (Lipoid S 45, Lipoid, Ludwigshafen, Germany), Kolliphor® EL (BASF, Ludwigshafen, Germany), glycerol (T.T.T., Sveta Nedjelja, Croatia), low molecular weight (M_w) chitosan (M_w range 50–190 kDa, degree of deacetylation range 75–85% and viscosity range of 1% (*w/w*) solution in 1% acetic acid 20–300 mPas; Sigma-Aldrich, Steinheim, Germany) and medium M_w chitosan (M_w range 190–310 kDa, degree of deacetylation range 75–85% and viscosity range of 1% (*w/w*) solution in 1% acetic acid 200–800 mPa s; Sigma-Aldrich). Porcine gastric mucin type II was purchased from Sigma-Aldrich and 3-(4,5-dimethylthiazol-2-yl)-2,5-diphenyl tetrazolium bromide (MTT) was purchased from AppliChem (Darmstadt, Germany). Fluorescein sodium salt was purchased from Sigma-Aldrich, HEPES from AppliChem, $Na_2HPO_4 \cdot 2H_2O$ from Fluka Chemie AG (Buchs, Switzerland). All other reagents were of analytical grade and purchased from Kemig or Sigma-Aldrich. Simulated tear fluid (STF) pH 7.4 was prepared by dissolving KCl (1.4 mg mL^{-1}), NaCl (6.8 mg mL^{-1}), NaHCO$_3$ (2.2 mg mL^{-1}) and CaCl$_2 \cdot 2H_2O$ (0.08 mg mL^{-1}) in double-distilled water. Hank's balanced salt solution (HBSS) pH 6.0 was prepared by dissolving KCl (0.4 mg mL^{-1}), NaHCO$_3$ (0.35 mg mL^{-1}), NaCl (8.0 mg mL^{-1}), D-glucose monohydrate (1.1 mg mL^{-1}), KH$_2$PO$_4$ (0.06 mg mL^{-1}), Na$_2$HPO$_4 \cdot 2H_2O$ (0.06 mg mL^{-1}), CaCl$_2 \cdot 2H_2O$ (0.185 mg mL^{-1}), MgCl$_2 \cdot 6H_2O$ (0.1 mg mL^{-1}), MgSO$_4 \cdot 7H_2O$ (0.1 mg mL^{-1}) and HEPES (7.15 mg mL^{-1}) in double-distilled water. Krebs-Ringer buffer (KRB) pH 7.4 was prepared by dissolving KCl (0.4 mg mL^{-1}), NaCl (6.8 mg mL^{-1}), NaHCO$_3$ (2.1 mg mL^{-1}), MgSO$_4 \cdot 7H_2O$ (0.4 mg mL^{-1}), D-glucose monohydrate (1.1 mg mL^{-1}), CaCl$_2 \cdot 2H_2O$ (0.52 mg mL^{-1}), NaH$_2$PO$_4 \cdot 2H_2O$ (0.158 mg mL^{-1}) and HEPES (3.575 mg mL^{-1}) in double-distilled water.

2.2. Solubility study

The solubility of ibuprofen in Miglyol® 812 and lecithin/Miglyol® 812 (1:50, *w/w*) solution was determined by adding an excess amount of drug to 5 g of oil or lecithin solution in oil and subsequent magnetic stirring at 25 °C during 48 h to reach equilibrium. Afterwards, the samples were centrifuged for 30 min at 1520·*g* and the supernatants

filtered through 0.2 μm Spartan™ regenerated cellulose filters (Whatman, United Kingdom). The samples were further diluted with methanol and ibuprofen concentration was analyzed using Ultra-Performance Liquid Chromatography (UPLC), as described in Section 2.13.

2.3. Nanoemulsion preparation

2.3.1. Nanoemulsions with lecithin and Kolliphor® EL

NEs with 5% (*w/w*) Miglyol® 812 and increasing amounts of lecithin (0.1–1.0%, *w/w*) were prepared using microfluidizer (Model M-110EH-30, Microfluidics®, Westwood, MA, USA). Before homogenization lecithin was dissolved in Miglyol® 812 at room temperature (RT) under magnetic stirring. Lecithin solution in Miglyol® 812 (oil phase) was added to water phase under magnetic stirring, and the mixture was further pre-homogenized with Ultra-Turrax® (IKA-Werke GmbH & Company, Staufen, Germany) during 5 min at 6000 rpm. The obtained coarse emulsion was then processed with microfluidizer under the pressure of 1000 bar and 10 cycles.

NEs with 5% (*w/w*) Miglyol® 812, 0.1% (*w/w*) lecithin and increasing amounts of Kolliphor® EL (0.25–2.5%, *w/w*) were prepared as described above using the water phase containing Kolliphor® EL.

Process parameters (pressure and number of cycles) were optimized on a coarse O/W emulsion containing 5% (*w/w*) Miglyol® 812, 0.1% (*w/w*) lecithin and 0.5% (*w/w*) Kolliphor® EL. The pressure and the number of cycles were varied in the range 400–1300 bar and 1–15, respectively. NE with the same composition was also prepared using high-pressure homogenizer (Panda Plus 2000®, GEA Niro Soavi, Parma, Italy) under the pressure of 1000 bar and 5 cycles.

2.3.2. Chitosan-coated nanoemulsions

Chitosan-coated NEs were prepared with two different methods using increasing amounts of low (LM_w) or medium (MM_w) M_w chitosan. In the first method, optimized uncoated NE prepared using microfluidizer (1000 bar, 5 cycles) was magnetically stirred with different amounts of 1% (*w/w*) chitosan (LM_w or MM_w) solution (filtered, prepared in 0.5%, *w/w* acetic acid). The final chitosan concentration ranged from 0.05 to 0.5% (*w/w*) while the concentration of Miglyol® 812 was fixed at 2.5% (*w/w*). In the second method, different amounts of 1% (*w/w*) chitosan (LM_w) solution were added to the aqueous Kolliphor® EL solution (water phase) prior phase mixing and processing on microfluidizer (1000 bar, 5 cycles). The final chitosan concentration in NEs was 0.05 and 0.3% (*w/w*) and the concentration of Miglyol® 812 was again fixed at 2.5% (*w/w*).

2.3.3. Ibuprofen-loaded nanoemulsions

Ibuprofen-loaded chitosan-coated and uncoated NEs were prepared by dissolving ibuprofen (0.2%, *w/w*) in the oil phase (lecithin solution in Miglyol® 812) at RT under magnetic stirring. Glycerol (2.5%, *w/w*) was added to the water phase to adjust NE tonicity. Uncoated ibuprofen-loaded NE was prepared as described above, using microfluidizer (1000 bar, 5 cycles). Chitosan-coated ibuprofen-loaded NEs were prepared using the second method described in Section 2.3.2.

2.4. Droplet size, size distribution and zeta-potential analysis

Droplet size, polydispersity index (PDI) and zeta-potential of NEs were measured by photon correlation spectroscopy (PCS) using Zetasizer Ultra (Malvern Instruments, Malvern, United Kingdom) at 25 °C. For that purpose NE samples were diluted 500 (droplet size and PDI) and 100 (zeta-potential) times (*V/V*) with 0.45 μm filtered double-distilled water and 10 mM NaCl solution, respectively. The detection angle used for droplet size and PDI measurement was 90°. A disposable folded capillary cell (DTS1070) was used for zeta-potential measurement.

2.5. Morphological analysis

Atomic force microscopy (AFM) was employed to determine the morphological properties and to confirm data obtained on droplet size and PDI by PCS. AFM was performed using AutoProbe CP-Research SPM (TM Microscopes-Bruker) with 90 μm large area scanner. Formulations were diluted with ultra-pure water 500 times (*V/V*), 10 μL of diluted sample was placed on circular mica substrate (Highest Grade V1 AFM Mica Discs, Ted Pella Inc., Redding, CA, USA) and dried in vacuum. Due to the nature of the samples, noncontact mode was applied. AFM measurements were performed in air, using noncontact probes Bruker Phosphorous doped silicon Tap300, model MPP-11123-10 with Al reflective coating and symmetric tip. Driving frequency of the cantilever was about 300 kHz. Both topography and "error signal" AFM images were taken and later analyzed using the software Image Analysis 2.2.0 (NT-MDT, Moscow, Russia).

2.6. pH, osmolarity and surface tension

The pH of NEs was determined using a Seven Multi pH/conductometer (Mettler Toledo, Columbus, OH, USA) at 25 °C. Osmolarity was determined by freezing point depression method (Advanced® 3D3 Single-Sample Osmometer, Advanced Instruments, Norwood, MA, USA). The surface tension measurements were performed with Krüss K-100C tensiometer (Hamburg, Germany). Surface tension values were determined employing Du Noüy ring method. All the measurements were made in triplicate at 25 °C using water circulating bath with temperature stability within 0.02 °C.

2.7. Ibuprofen entrapment efficiency

The amount of ibuprofen entrapped in the oil droplets was determined by ultrafiltration. A 2 mL aliquot of ibuprofen-loaded NE was transferred to the upper chamber of a centrifuge tube fitted with ultrafilter (Centricon®, NMWL 10 kDa, Merck-Millipore, Billerica, MA, USA), which was then centrifuged at 5000·*g* for 1 h. The entrapment efficiency (*EE* %) was calculated from the following equation:

$$EE\% = \frac{Wt - Wf}{Wt} \times 100 \tag{1}$$

where W_t is the total amount of ibuprofen in the NE and W_f is the amount of ibuprofen in the filtrate, which was determined by UPLC, as described in Section 2.13.

2.8. Stability studies

NEs were stored for 30 days at 4 and 25 °C, after which droplet size, PDI, zeta-potential and pH were measured to evaluate stability. Stress tests (heating–cooling cycles, centrifugation and freeze-thaw cycles) were performed as previously described (Shafiq et al., 2007). Six cycles between 4 and 45 °C were done with storage at each temperature not less than 48 h. Centrifugation was performed at 9000·*g* during 30 min. In the end, NEs were subjected to three freeze-thaw cycles between −20 and 25 °C with storage at each temperature not less than 48 h. After each cycle or centrifugation NEs were examined visually for phase separation and characterized in terms of droplet size, PDI and zeta-potential to evaluate stability. For each of the stress tests freshly prepared NE formulations were used.

2.9. Nanoemulsion sterilization

NEs were aseptically filtered through 0.2 μm polyethersulfone (PES) filter or autoclaved at 121 °C for 20 min. After each sterilization process NEs were examined visually for phase separation and characterized in terms of droplet size, PDI and zeta-potential.

2.10. In vitro ibuprofen release

In vitro ibuprofen release was determined using US Pharmacopeia apparatus type II (708-DS Dissolution Apparatus, Agilent Technologies, Santa Clara, CA, USA) modified by the addition of a cellulose acetate dialysis bag (Spectra/Por1 4 Dialysis Tubing, MWCO 12–14 kDa, Medicell International Ltd, London, UK). NE sample (1 mL) was placed in the dialysis bag, the bag was sealed and tied to the apparatus paddle and immersed in 900 mL of phosphate buffer pH 7.4 (34 °C, 50 rpm). At scheduled time intervals, 2 mL aliquots were withdrawn and replaced with fresh dissolution medium. The samples (including donor compartments at the end of the experiment) were analyzed for ibuprofen content by UPLC method, as described in Section 2.13. All experiments were performed at least in triplicate.

2.11. Mucoadhesive properties

NE mucoadhesive properties were determined by a slightly modified simple rheological method (Hassan and Gallo, 1990) using MCR 102 rheometer (Anton Paar, Graz, Austria) equipped with a cone-plate measuring device (CP 50-1, trim position 102 μm). For this purpose a 20% (*w/w*) mucin dispersion in STF was prepared by overnight magnetic stirring at RT. Mucin dispersion (10%, *w/w*) with or without NE was prepared by the addition of NE or water in 1:1 (*w/w*) ratio in the 20% (*w/w*) mucin dispersion in STF. The resulting mixtures were magnetically stirred at 750 rpm during 15 min, and subsequently left without stirring for 1 h at RT before measurement. NEs mixed with STF in 1:1 (*w/w*) ratio were prepared in the same way. Flow curves of all samples were measured at the shear rate range 0.1–100 s^{-1} and 34 °C. To calculate the viscosity component due to bioadhesion (η_b) viscosity values at the shear rate of 100 s^{-1} were used and η_b was calculated from the equation:

$$\eta_b = \eta_t - \eta_m - \eta_n \tag{2}$$

where η_t is viscosity of the measured sample, η_m viscosity of 10% (*w/w*) mucin dispersion and η_n viscosity of NE mixed with STF in 1:1 (*w/w*) ratio. All measurements were performed in triplicate.

2.12. Biocompatibility studies

2.12.1. In vitro corneal biocompatibility

Human corneal epithelial cells (HCE-T, RIKEN Cell Bank, Tsukuba, Japan) were used for cultivation of 3D HCE-T cell-based model as previously described (Juretic et al., 2017). Briefly, Transwell® polycarbonate membrane cell culture inserts (0.4 μm pore size, 12 mm diameter, surface area 1.12 cm^2, Corning B.V. Life Sciences, Amsterdam, The Netherlands) were coated with rat tail type I collagen (225 μg per well; Sigma-Aldrich) and human fibronectin (4 μg per well; Sigma-Aldrich). HCE-T cells suspended in supplemented DMEM/F12 (Sigma-Aldrich) medium (Juretic et al., 2017) (10^5 cells in 0.5 mL) were seeded onto the coated polycarbonate filter, and 1.5 mL of the culture medium was added to the basolateral side. The cells were cultivated submerged in the medium until a sharp increase in transepithelial electrical resistance (TEER) was observed (from 4 to 7 days), after which they were exposed to the air-liquid interface (ALI) for the following 3 days. The culture medium was changed every 2 days during the submerged conditions and every day during the exposure to the ALI. During the ALI exposure, the inserts were lifted on a metal plate to increase the basolateral volume to 2 mL.

Before treatment with the NE samples, the medium was aspirated from the basolateral side, the metal plate was removed and the inserts were washed with HBSS. The inserts were then transferred to a new 12-well cell culture plate (Corning B.V. Life Sciences) and incubated for 30 min in HBSS (0.5 mL apical side/1.5 mL basolateral side) at 37 °C. After incubation, HBSS from the apical side was removed and 0.5 mL of NE sample diluted 10 times (*V/V*) in HBSS pH 6.0, as previously

described (Kinnunen et al., 2014), was added and the model was incubated for 30 min at 37 °C. HBSS only and ibuprofen suspension (0.2 mg mL^{-1}) in HBSS were used as controls. All the samples were tested in triplicate. The pH of HBSS was set to 6.0 in order to ensure protonated form of chitosan on the NE droplet surface (Rinaudo, 2016). After incubation the test samples were removed from the apical side, the inserts were washed with HBSS and displaced to a new 12-well plate with the metal plate and 2 mL of medium at the basolateral side. MTT assay was performed after 24 h according to the protocol by Pauly and coworkers (Pauly et al., 2009). The medium was removed and 0.7 mL of MTT solution in the medium (0.5 mg mL^{-1}) was added to both apical and basolateral side and the cell model was incubated for 3 h at 37 °C. Subsequently, the MTT solution was removed and formazan crystals were dissolved by the addition of 0.7 mL of isopropanol (Kemig) to both sides. The absorbance was measured at 570 nm with a microplate reader (1420 Multilabel counter VICTOR[3], Perkin Elmer, Waltham, MA, USA).

2.12.2. Ex vivo corneal biocompatibility

Corneal biocompatibility was assessed on freshly excised porcine corneas. Briefly, fresh porcine eyeballs were obtained from Large White pigs (age 6–7 months, weight 90–115 kg, both female and male animals) from a local slaughterhouse. Porcine eyeballs were enucleated, rinsed with an isotonic saline solution (NaCl 0.9%; B. Braun, Melsungen, Germany) and transported in cold KRB buffer in a container held on ice. After transport, the eyeballs were submerged in 1% Betadine® solution (Alkaloid, Skopje, North Macedonia) for 3–5 min for microbial decontamination and subsequently washed with phosphate buffered saline pH 7.4 (PBS; Sigma-Aldrich) containing 1% (*V/V*) penicillin/streptomycin/amphotericin B mixture (Cat. No. 17-745E; Lonza, Basel, Switzerland). The transport of porcine eyeballs and the excision of corneo-scleral buttons were performed within 2 h of animal death. The corneas were excised as corneo-scleral buttons in a laminar-flow hood (Thermo Scientific, Waltham, MA, USA) and placed with the epithelial side down on 15 mL conical centrifuge tube caps. 1 mL of 4% (*w/V*) agar (Muller Hinton II Agar, BBL™, Becton, Dickinson and Company, Sparks, MD, USA) in DMEM/F-12 (Gibco®, Life Technologies™, Carlsbad, CA, USA) cell culture medium without supplements, previously autoclaved (121 °C, 20 min) and if necessary reheated in a microwave to a liquid state was pipetted on endothelial side of each corneo-scleral button, in order to enable the formation of a naturally curved shape of the corneas. After cooling and subsequent gelling of the agar solution the corneo-scleral buttons were placed on a 6-well plate (endothelial side down) and 3.5 mL of DMEM/F-12 (Gibco®, Life Technologies™), supplemented with 10% (*V/V*) FBS (Biosera, Boussens, France) and 10% (*V/V*) penicillin/streptomycin/amphotericin B mixture was added to each well, so that the corneas were exposed to the air. The corneo-scleral buttons were left overnight in the incubator (humidified atmosphere, 5% CO$_2$, 37 °C) and treatment with the NE samples was done the following day. The medium was aspirated and custom-made silicone rings were placed onto the corneas. 200 μL of a test sample was added inside each ring and the corneas were incubated at 37 °C for 5 and 15 min. After each time-point the samples were removed, the corneas were washed with PBS and the extent of any corneal damage was evaluated visually with the aid of fluorescein solution (2 mg mL^{-1}) in PBS and a cobalt-blue lamp (Conóptica, Barcelona, Spain). Briefly, the silicone rings were placed on the corneas again and 200 μL of the fluorescein solution was put inside and left for 20 s. The fluorescein solution was removed, the corneas were washed with PBS and photographs were taken through a yellow filter of the cobalt-blue lamp. PBS was used as negative control, while acetone (Sigma-Aldrich), 0.1 M NaOH solution and 0.025% (*w/V*) benzalkonium chloride (BAK; Sigma-Aldrich) solution in PBS were used as positive controls. All the samples were tested in triplicate.

2.13. Quantification

The quantitative determination of ibuprofen was performed by UPLC using an Agilent Infinity 1290 (Agilent) with the Acquity UPLC BEH Shield RP18 Column (1.7 μm, 2.1 mm × 50 mm) (Waters, Milford, MA, USA) and isocratic elution. For ibuprofen solubility study ibuprofen solutions in oil were diluted with methanol. The mobile phase was composed of NaH_2PO_4 buffer (prepared in in Milli-Q™ water (Merck-Millipore), 1.2 mg mL^{-1}, pH 2.5) and acetonitrile (ACN; Merck-Millipore) in 60:40 (*V/V*) ratio. The following UPLC conditions were applied: column temperature 50 °C, flow rate 0.4 mL min^{-1}, injection volume 4 μL, detection wavelength 225 nm. For ibuprofen entrapment efficiency the filtrates were analyzed without dilution. The following UPLC conditions were applied: mobile phase buffer:ACN in 65:35 (*V/V*) ratio, column temperature 50 °C, flow rate 0.8 mL min^{-1}, injection volume 4 μL, detection wavelength 225 nm. For ibuprofen quantification in *in vitro* release samples, different methods were used for receptor and donor compartment sample analysis. The receptor compartment samples were analyzed using the same method as for ibuprofen entrapment efficiency analysis, with the only difference in the injection volume which was 20 μL. The donor compartment samples were diluted with methanol prior analysis and then analyzed with the method used for ibuprofen solubility study. All samples and standard solutions were filtrated through 0.2 μm Spartan™ regenerated cellulose filters prior analysis. For each sequence standard solutions were prepared in duplicate and injected alternately. At least five standard solution injections were done in each injection sequence. System suitability was evaluated according to the following criteria: relative standard deviation (RSD) of the detector response factor for all standard solution injections in the sequence is not more than 2.0% and tailing factor of ibuprofen peak is not more than 1.5. The UPLC methods were validated in terms of linearity, accuracy and repeatability. The methods were found to be linear ($R^2 \geq 0.99$), accurate (recovery values 98–102%) and repeatable (relative standard deviation of peak area (RSD) $\leq$ 2.0%).

2.14. Statistical analysis

Statistical analyses were performed on the data obtained from the study on mucoadhesion and *in vitro* biocompatibility using One-way ANOVA followed by a multiple comparisons Tukey's and Dunnett's post hoc test, respectively with $P < 0.05$ set as the minimal level of significance. Calculations were performed with the GraphPad Prism software (GraphPad Software, Inc., San Diego, USA; www.graphpad.com).

Ibuprofen *in vitro* release profiles from the tested NEs and controls were compared by the similarity factor (f_2) calculation, as previously described (Diaz et al., 2016). The mean cumulative amounts of the released drug from the two formulations were compared at each time point. The release profiles were considered similar when $f_2 > 50$.

3. Results and discussion

Ophthalmic NEs are complex dosage forms with several physicochemical parameters, such as nanodroplet size, size distribution and zeta-potential, formulation viscosity profile as a function of applied shear, pH, osmolarity, and surface tension, affecting their *in vivo* performance (Qu et al., 2018; Walenga et al., 2019). Although NEs are complex, they can be easily manufactured on a large scale using specific equipment, such as microfluidizers and high-pressure homogenizers, and sterilized by filtration or autoclavation. Formulation parameters (type and concentration of excipients) as well as process parameters (homogenization pressure and number of homogenization cycles) are the determinants of formulation physicochemical parameters, but specifically for the treatment of DED, formulation parameters are possibly the key determinants of formulation effect on the tear film stability. In clinical studies of CsA NE, a significant improvement over the baseline

for several *in vivo* outcome measures was indicated for formulation without API (Simmons and Vehige, 2007; Stevenson et al., 2000; Walenga et al., 2019). Moreover, studies that measured tear film breakup time (TBUT), a metric of tear film stability defined as the time from the opening of the eyelids to the initial dry spot formation, showed an increase in TBUT 1 h after instillation of an artificial tear product with composition similar to Restasis® (Simmons and Vehige, 2007). The long residence time of the lipid components, detected 3 to 4 h after instillation, may be the cause of TBUT enhancement (Stevenson et al., 2000; Walenga et al., 2019). Therefore, special emphasis should be placed on the selection of excipients in order to obtain a functional NE for DED treatment.

3.1. Excipient and formulation considerations

While in primary NEs oil phase is emulsified with water phase using a surfactant, in secondary NEs an oppositely charged polyelectrolyte is deposited over a primary NE droplet surface (Rai et al., 2018). To obtain positively charged secondary NEs, we selected chitosan as the positively charged polyelectrolyte and Lipoid S 45 lecithin as the anionic surfactant enabling interaction with chitosan (Hafner et al., 2009). Moreover, Lipoid S 45 lecithin is a fat-free soybean lecithin with 45% (*w/w*) phosphatidylcholine and 10–18% (*w/w*) phosphatidylethanolamine, two constituents of the natural tear film important for its stability. Moreover, studies suggest that lower levels of the two polar phospholipids are present in individuals with tear film deficiencies (Jones et al., 2017; McCulley and Shine, 1997; Shine and McCulley, 1998).

The selection of the internal oil phase depends on the compatibility of the oil with lecithin and on the solubility of the drug in the oil, especially because the oil phase concentration in the eye drops should not exceed 5% (Tamilvanan and Benita, 2004). In this study, among ophthalmically acceptable oils tested (castor oil, soybean oil, sesame oil), lecithin was easily soluble without heating only in Miglyol® 812, a medium-chain-triglyceride (MCT) oil consisting of a mixture of triglycerides of saturated fatty acids. Furthermore, ibuprofen was also shown to have high solubility in Miglyol® 812 (92.7 $\pm$ 0.2 mg g^{-1}) and Miglyol® 812/lecithin (50:1, *w/w*) solution (101.3 $\pm$ 3.3 mg g^{-1}).

A total of 5 NE formulations of Miglyol® 812 (5%, *w/w*) and lecithin (0.1, 0.25, 0.5, 0.75 and 1%, *w/w*) were prepared by microfluidization under the pressure of 1000 bar and 10 cycles (Table 1). The resulting NEs were highly fluid and homogenous with milky-white appearance, characterized with droplet size from 251.6 to 140.1 nm, PDI from 0.100 to 0.174 and zeta-potential from −40.1 to −48.8 mV with increasing the amount of lecithin in the formulation. At this point, the concentration of lecithin adequate to render the droplets negatively charged was to be determined and, as it can be seen from Table 1, all the NEs prepared had highly negative zeta-potential. The most important criterion in manufacturing NEs is to obtain a desired droplet size with monomodal distribution. The mean droplet size expectedly decreased with the increase in the amount of lecithin, but with lecithin concentrations higher than 0.75% (*w/w*) PDI started to increase. Even though the NE produced with the lowest concentration of lecithin (0.1%, *w/w*) had the largest mean droplet size, it was chosen for further

Table 1

Droplet size, PDI and zeta-potential of NEs with 5% (*w/w*) Miglyol® 812 and increasing amounts of lecithin.

Lecithin (%, *w/w*)	Droplet size (nm)	PDI	Zeta-potential (mV)
0.1	251.6 $\pm$ 1.6	0.100 $\pm$ 0.016	−40.1 $\pm$ 1.5
0.25	220.1 $\pm$ 2.4	0.089 $\pm$ 0.018	−44.9 $\pm$ 1.3
0.5	184.8 $\pm$ 1.2	0.116 $\pm$ 0.008	−46.9 $\pm$ 1.0
0.75	160.1 $\pm$ 1.9	0.112 $\pm$ 0.010	−48.9 $\pm$ 1.2
1.0	140.1 $\pm$ 2.5	0.174 $\pm$ 0.048	−48.8 $\pm$ 1.2

Values are mean $\pm$ SD ($n = 2$).

Table 2

Droplet size, PDI and zeta-potential of NEs with 5% (*w/w*) Miglyol® 812, 0.1% (*w/w*) lecithin and increasing amounts of Kolliphor® EL.

Kolliphor® EL (%, *w/w*)	Droplet size (nm)	PDI	Zeta-potential (mV)
0.25	212.3 ± 3.8	0.112 ± 0.017	−20.7 ± 0.7
0.5	181.1 ± 2.9	0.092 ± 0.026	−15.9 ± 0.4
1.0	138.6 ± 1.8	0.108 ± 0.017	−13.0 ± 0.4
2.0	99.1 ± 1.9	0.176 ± 0.019	−6.2 ± 0.6
2.5	83.6 ± 1.2	0.201 ± 0.018	−3.6 ± 0.3

Values are mean ± SD (*n* = 2).

formulation development studies because its zeta-potential was already highly negative, and another non-ionic surfactant was to be introduced for further droplet size reduction and stabilization.

It has already been demonstrated that a combination of lecithin with a second more hydrophilic surfactant can lead to formation of NEs with decreased droplet size and increased stability, even in the presence of an API (Trotta et al., 2002). Therefore, Kolliphor® EL was included as the second, more hydrophilic surfactant, as it is approved in ophthalmic formulations by the FDA in concentrations up to 5% (FDA Database: Inactive ingredients). A total of 5 NE formulations of Miglyol® 812 (5%, *w/w*), lecithin (0.1%, *w/w*) and Kolliphor® EL (0.25, 0.5, 1, 2 and 2.5%, *w/w*) were prepared by microfluidization (Table 2). The addition of Kolliphor® EL in NE with lecithin caused an expected droplet size reduction. Even though a slight increase in PDI was noticed with Kolliphor® EL concentrations higher than 1% (*w/w*), all NEs had PDI ≤ 0.200 and were therefore considered to be monodisperse (Klang and Valenta, 2011). Most importantly, the addition of Kolliphor® EL had a major influence on NE zeta-potential; the zeta-potential values were approaching zero with the increase in Kolliphor® EL concentration. The presence of the non-ionic surfactant, Kolliphor® EL on the droplet surface probably reduced the density of negatively charged molecules from lecithin packed on the droplet surface. Thus, to decide which formulation should be selected for further studies, a compromise was made between the lowest droplet size and PDI and a zeta-potential negative enough to enable electrostatic interaction with positively charged chitosan molecules. NE with 0.5% (*w/w*) Kolliphor® EL with droplet size 181.1 ± 2.9 nm, PDI of 0.092 ± 0.026 and zeta-potential of −15.9 ± 0.4 mV was chosen for further studies.

After optimizing the formulation parameters (i.e. the concentration of lecithin and Kolliphor® EL), optimization of process parameters was performed. The homogenization pressure and the number of cycles (passes of the formulation through microfluidizer) were gradually increased and the results are graphically shown in Fig. S1. In accordance with previously reported data (Meleson et al., 2004; Uluata et al., 2016), the formulation droplet size and PDI decreased with increasing homogenization pressure and number of cycles, while the zeta-potential remained practically unchanged through all the conditions applied. However, no further droplet size (and PDI) reduction was achieved

when the homogenization pressure was increased to 1300 bar. Therefore, the homogenization pressure of 1000 bar was chosen for further studies. Even though only a minor droplet size reduction (3.6 nm) was achieved when the number of cycles under this pressure was increased from 3 to 5, we decided to use 5 cycles for further NE preparation to assure sufficient homogenization of the formulations. The same optimized formulation was prepared under the selected process parameters (1000 bar, 5 cycles) using a high-pressure homogenizing device and similar results (droplet size, PDI, zeta-potential) were obtained (Fig. S2), which indicates that preparation of the formulation could be transferable to high-energy methods other than microfluidization.

The cationic polysaccharide chitosan was chosen to form a coating around the oil droplets making them positively charged and therefore mucoadhesive. The selection of chitosan was also based on its biocompatibility and biodegradability since it can be degraded by lysozyme which is highly concentrated in tears (de la Fuente et al., 2010). Additionally, the antimicrobial properties of chitosan could be very advantageous for patients with DED who often suffer secondary infections (de la Fuente et al., 2010). To obtain chitosan-coated secondary NEs, we screened the effect of addition of LM_w and MM_w chitosan solution to the prepared NE under magnetic stirring. The final chitosan concentration ranged from 0.05 to 0.5% (*w/w*). Since chitosan was added as 1% (*w/w*) solution, the concentration of other NE components (oil and surfactants) decreased. To assure the same nanodroplet surface area available for coating with chitosan molecules, the concentration of Miglyol® 812 was set to 2.5% (*w/w*) in all the formulations by the addition of double-distilled water where necessary. Chitosan-coated NEs prepared with LM_w chitosan had lower droplet size and PDI values than those prepared with MM_w chitosan (Table 3), which can be explained by a thinner coating layer formed by chitosan with lower M_w (Li et al., 2016). Chitosan M_w did not seem to have a strong influence on the final NE zeta-potential, as already reported (Mun et al., 2006). Therefore, LM_w chitosan was chosen for further formulation optimization in low and high concentration (0.05 and 0.3%, *w/w*) resulting with zeta-potential of 29.2 ± 0.2 and 40.3 ± 0.9 mV, respectively. Further step was the addition of chitosan in the aqueous phase prior phase mixing and processing on microfluidizer. The comparison between chitosan-coated NEs obtained with the two different methods is shown in Table 4. A decrease in NE mean droplet size, zeta-potential and PDI is evident when chitosan is added prior processing on microfluidizer. The moment of chitosan addition to the formulation seemed to have a major impact on the final NE characteristics. The observed decrease in droplet size, PDI and zeta-potential could be a consequence of intercalation of chitosan molecules between surfactant molecules at the droplet surface and a mixed interfacial film formation with overall positive surface charge (Jumaa and Muller, 1999). The NE formulation with higher chitosan concentration had higher PDI, which was expected because chitosan products show a broad range of molecular weights (Nguyen et al., 2009). The morphological AFM analysis was performed as a complementary method to confirm the results obtained by PCS. The

Table 3

Droplet size, PDI and zeta-potential of NEs with 2.5% (*w/w*) Miglyol® 812, 0.05% lecithin, 0.25% (*w/w*) Kolliphor® EL and different chitosan (low (LM_w) and medium molecular weight (MM_w)) concentrations.

Chitosan (%, *w/w*)	LM_w			MM_w		
	Droplet size (nm)	PDI	Zeta-potential (mV)	Droplet size (nm)	PDI	Zeta-potential (mV)
0.05	199.6 ± 1.6	0.072 ± 0.002	29.2 ± 0.2	255.9 ± 44.7	0.240 ± 0.066	31.8 ± 1.3
0.1	199.3 ± 4.5	0.138 ± 0.052	32.7 ± 0.1	282.6 ± 9.6	0.305 ± 0.003	35.3 ± 1.0
0.2	279.0 ± 28.4	0.288 ± 0.001	37.4 ± 0.0	418.7 ± 139.3	0.652 ± 0.039	38.9 ± 1.6
0.3	360.9 ± 14.7	0.489 ± 0.013	40.3 ± 0.9	583.7 ± 36.1*	0.841 ± 0.023	41.4 ± 2.4
0.4	390.1 ± 27.4	0.504 ± 0.014	39.0 ± 0.5	626.8 ± 74.3*	0.853 ± 0.065	42.2 ± 2.2
0.5	325.7 ± 15.0	0.535 ± 0.070	42.7 ± 1.6	749.4 ± 27.7*	0.791 ± 0.175	44.0 ± 2.0

Values are mean ± SD (*n* = 2).

* The result may not represent the real mean value due to very high PDI (> 0.7).

Table 4

Comparison of LM$_w$ chitosan coated NEs prepared with two different methods described in Section 2.3.2.

Chitosan (%, *w/w*)	Chitosan added after microfluidization			Chitosan added before phase mixing		
	Droplet size (nm)	PDI	Zeta-potential (mV)	Droplet size (nm)	PDI	Zeta-potential (mV)
0.05	199.6 ± 1.6	0.072 ± 0.002	29.2 ± 0.2	179.3 ± 2.3	0.061 ± 0.015	18.7 ± 1.9
0.3	360.9 ± 14.7	0.489 ± 0.013	40.3 ± 0.9	179.3 ± 7.6	0.169 ± 0.011	30.0 ± 1.5

Values are mean ± SD ($n = 2$).
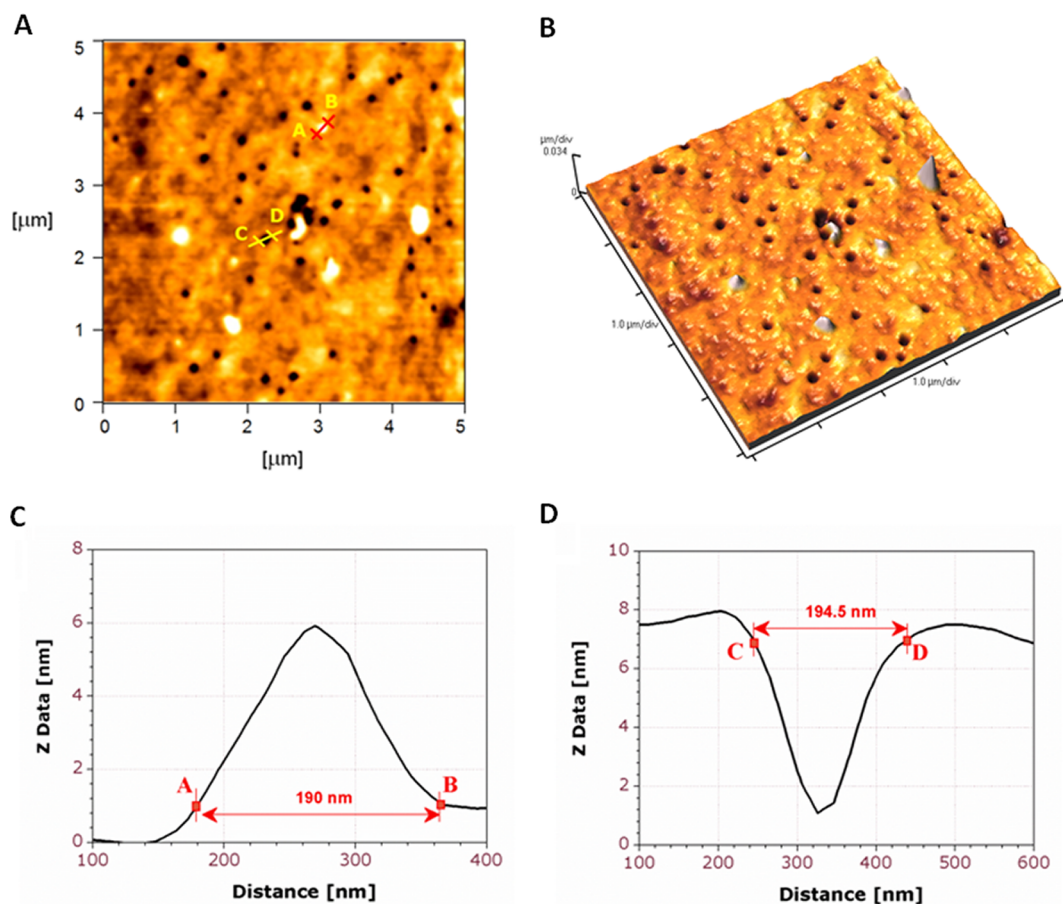
Fig. 1. AFM images of NC2 formulation (0.3%, *w/w* LM$_w$ chitosan, 2.5%, *w/w* Miglyol® 812, 0.05%, *w/w* lecithin and 0.25%, *w/w* Kolliphor® EL): (a) 2D topography (5 × 5 μm scan area); (b) 3D topography (5 × 5 μm scan area); (c) and (d) profiles of two representative NE droplets marked on the 2D topography (a).

analysis pointed out spherical droplets with dimensions similar to those obtained with PCS measurements (Fig. 1). Thus, the second preparation method where the addition of chitosan to the formulation is done before processing on microfluidizer was used in further studies, leading to the lowest droplet size and PDI of chitosan-coated NEs.

Optimized chitosan-coated NEs with 0.05 (NC1) and 0.3 (NC2) % (*w/w*) chitosan, and the uncoated control formulation (N) stored in ambient or refrigerated conditions over 30 days did not show any significant differences in their appearance. However, in comparison to freshly obtained formulations a certain decrease in PDI was observed, especially after 30-day storage at 25 °C (Fig. 2). NC1 did not show major changes in droplet size, but the droplet size of NC2 notably increased after 30-day storage at 25 °C. A small increase in zeta-potential was also observed for NC2 formulation stored at 25 °C. Acceptable stability was further studied with special thermodynamic stability tests, which predict droplet integrity in case of temperature fluctuations (6 cycles of refrigeration and heat, 3 freeze-thaw cycles) (Fig. 3). NC1 and NC2 remained visually unchanged showing no phase separation. Heating-cooling cycles caused certain droplet size increase in NC2 (approximately 1.6 times), with noticeable PDI fluctuations, but

without significant changes in zeta-potential. On the other hand, heating-cooling cycles did not cause notable changes in the formulations N and NC1 Three freeze-thaw cycles showed negligible effect on droplet size and zeta-potential of all NEs tested, with certain PDI increase in NC2. Kinetic instability such as creaming, settling or any other form of phase separation was ruled out by centrifugation of the formulations at 9000·*g*. After centrifugation an apparent phase separation was observed in all the formulations, but after only a mild agitation the formulations turned uniform again, which was also confirmed by droplet size, PDI and zeta-potential measurements (Fig. 3). Although these stability studies demonstrated superior stability of NC1 over the NC2 formulation, none of the formulations showed creaming or phase separation after 30-day storage or stress tests, which was the prerequisite for ibuprofen introduction.

3.2. Loading of chitosan-coated NEs with ibuprofen and their optimization for topical ophthalmic administration

In ophthalmic formulations, ibuprofen is used at low concentrations (between 0.1 and 0.2%, *w/w*). Ibuprofen-loaded NEs were prepared by
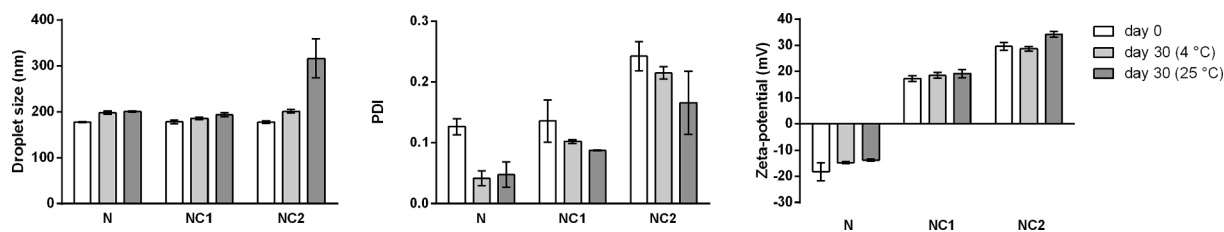
Fig. 2. Droplet size, PDI and zeta-potential of chitosan-coated NEs with 0.05 (NC1) and 0.3 (NC2) % (*w/w*) chitosan, and the uncoated control formulation (N) measured after preparation and 30-day storage at 4 or 25 ˚C. NEs were prepared by adding chitosan to water phase before phase mixing and microfluidization. Data are expressed as mean ± SD (*n* = 2–3).

ibuprofen dissolution in the oil phase prior phase mixing and the final NE composition is shown in Table 5. In addition to ibuprofen incorporation in the oil phase, in this step of chitosan-coated NE optimization, formulation tonicity was adjusted by the addition of glycerol in the aqueous phase. Glycerol was chosen as the tonicity agent not to induce significant alterations in the physicochemical properties of the chitosan-coated NEs (Teixeira et al., 2017) and also due to its short-lasting osmoprotective effect (Baudouin et al., 2013).

Ibuprofen is a weak acid, BCS class II compound, and its molecules are well encapsulated into the oil droplets due to the hydrophobic character of the drug (Gue et al., 2016). Ibuprofen entrapment efficiency was higher than 98% in all the NEs (Table 6). Droplet size and PDI remained similar after ibuprofen incorporation, but the zeta-potential of chitosan-coated INC1 and INC2 formulations was slightly higher than for unloaded NC1 and NC2 formulations (Table 6). *In vivo* performance of ophthalmic NEs is further affected by the formulation pH, surface tension and viscosity profile as the function of the applied shear. The pH of all the chitosan-coated NE formulations was around 4.5 regardless of ibuprofen incorporation (Table 6), due to the acetic acid addition necessary to dissolve chitosan. Wide pH range can be

tolerated by the ocular surface, especially when the ophthalmic product is not buffered (Lang et al., 2005; Fialho and da Silva-Cunha, 2004). A study performed on 6 healthy volunteers showed that immediately after the instillation of 20 μL of 0.067 M phosphate-buffered saline, pH 5.5, the pH value of the tear film was found to be about 6.0–6.5 and that the tear film rapidly became more alkaline, reaching pH 7 in about 1 min, and approximately its normal value in an additional 1–1.5 min (Yamada et al., 1998) It is generally accepted that low pH of an ophthalmic product will not necessarily cause stinging or discomfort upon instillation if the pH of the tears can be rapidly brought back to normal values (Lang et al., 2005), but data about the buffering capacity of tears in DED are lacking. However, there are studies that indicate slightly higher pH of tears of participants with DED (Khurana et al., 1991; Norn, 1988). Even though DED patients often have lower tear volume, this alkaline shift might be a compensatory mechanism to return the pH of tears to more neutral values after instillation of an acidic ophthalmic product, as it is the case with chitosan-coated NEs.

Surface tension is an important physicochemical formulation parameter that determines spreading of a formulation across the ocular surface and also influences capillary drainage through the nasolacrimal
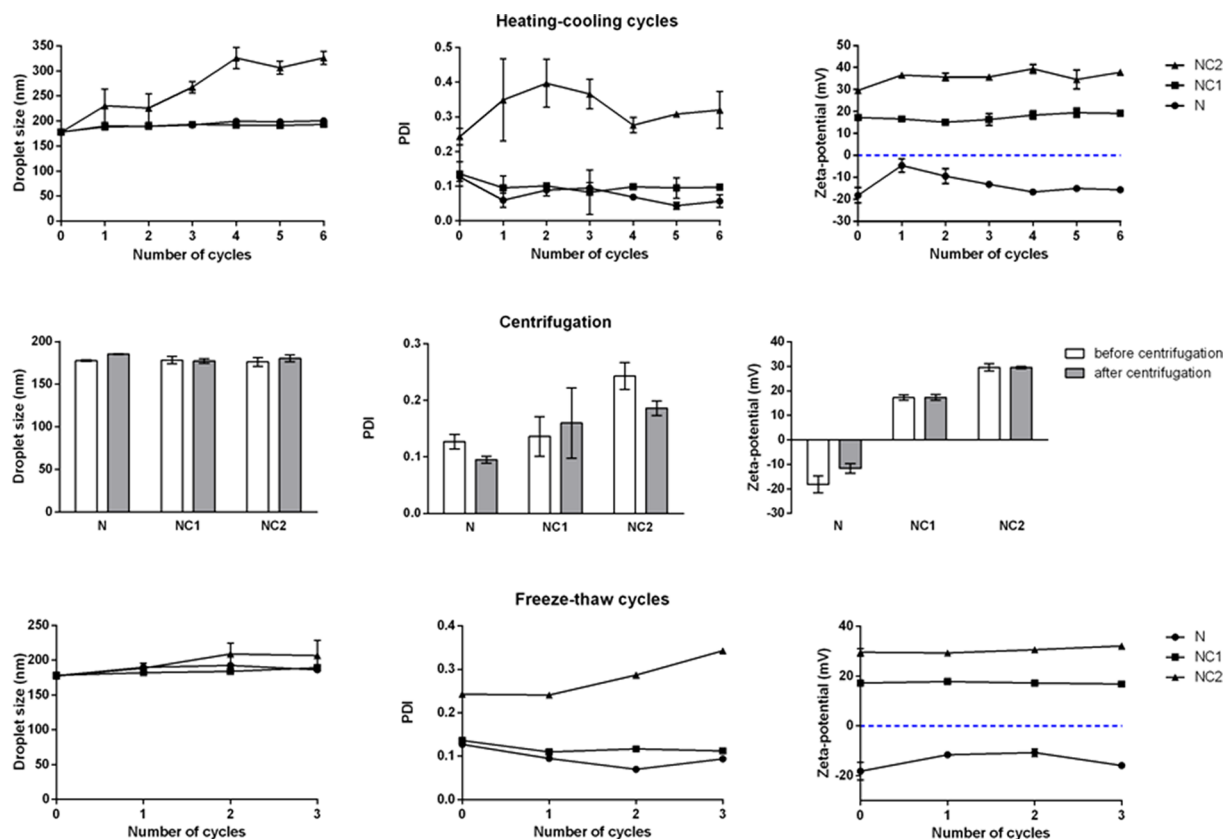

Fig. 3. Droplet size, PDI and zeta-potential of chitosan-coated NEs with 0.05 (NC1) and 0.3 (NC2) % (*w/w*) chitosan, and the uncoated control formulation (N) measured before and after stress tests (heating-cooling cycles, centrifugation and freez-thaw cycles). Data are expressed as mean ± SD (*n* = 2–3).

Table 5
The final NE composition.

Formulation	Ibuprofen (%, *w/w*)	Chitosan LM$_w$ (%, *w/w*)	Miglyol® 812 (%, *w/w*)	Lecithin (%, *w/w*)	Kolliphor® EL (%, *w/w*)	Glycerol (%, *w/w*)	Water (%, *w/w*)
N	–	–	2.5	0.05	0.25	2.5	94.7
IN	0.2	–	2.5	0.05	0.25	2.5	94.5
NC1	–	0.05	2.5	0.05	0.25	2.5	94.65
INC1	0.2	0.05	2.5	0.05	0.25	2.5	94.45
NC2	–	0.3	2.5	0.05	0.25	2.5	94.4
INC2	0.2	0.3	2.5	0.05	0.25	2.5	94.2

ducts, affecting precorneal residence time of the instilled formulation. All the surface tension measurements were carried out at the eye drop application temperature, i.e. 25 °C, to be comparable with the tear film surface tension values reported, which were also measured at 25 °C. Chitosan and ibuprofen both induced a decrease in the formulation surface tension (Table 6). Surface active properties of chitosan are well-known, as it can be used as an O/W emulsion stabilizer (Payet and Terentjev, 2008). Ibuprofen surface active properties have also been confirmed (Baydoun et al., 2004; Rao et al., 1992) and are probably the reason for additional surface tension decrease when ibuprofen was introduced to the chitosan-coated NEs. The surface tension at the air interface of the preocular tear film has physiological range of 40–46 mN m^{-1}, while in DED the characteristic range is approximately 44–53 mN m^{-1} (Nagyova and Tiffany, 1999). In general, higher surface tension values coincide with lower tear film stability, but the scarce literature data reported that the eye drops with a surface tension below 35 mN m^{-1} are painful and uncomfortable (Hotujac Grgurevic et al., 2017; Ludwig and Reimann, 2015). Higher concentration of chitosan in the INC2 formulation pushed the surface tension slightly below this limit.

Viscosity profile as the function of the applied shear showed a Newtonian fluid behavior of the NEs. The measured viscosity values were similar to the viscosity of water, with a slight increase with the addition of chitosan (1.1–4.1 mPa s, Table 6). The measured viscosity values were in the physiological range of a human tear film (1–9 mPa s) (Pandit et al., 1999; Tiffany, 1991), which has been proposed as the desirable viscosity range for the artificial tears that follow Newtonian behaviour (Acar et al., 2018). Moreover, low formulation viscosity enables dosing accuracy and ease of eye-drop administration.

Tear film hyperosmolarity plays etiological role in DED and osmoprotectants could provide necessary protection of cells under extreme osmotic stress by balancing the osmotic pressure without disturbing cell metabolism (Jones et al., 2017). Osmolarity of all ibuprofen-loaded NEs was in the osmolarity range of a normal tear film (Table 6), i.e. between 270 and 315 mOsm kg^{-1} (Willcox et al., 2017).

After 30-day storage at 4 °C INC1 and the control chitosan-uncoated formulation IN showed only a minor droplet size increase of 8.2 and 5.3 nm, respectively, while PDI and zeta-potential values remained unchanged or very similar (INC1: 0.127 ± 0.016, 22.8 ± 2.3 mV; IN: 0.101 ± 0.008, −12.2 ± 1.8 mV). However, a significant droplet size increase of 35.3 nm (18%) was noted for INC2 formulation, while its PDI and zeta-potential remained quite similar to those of the freshly-prepared INC2 formulation (0.323 ± 0.034, 38.9 ± 1.4). Overall, it seems that the addition of ibuprofen caused a detectable instability of the INC2 formulation. On the contrary, stability of the INC1 formulation with lower chitosan concentration was not compromised. The pH of all the formulations remained practically unchanged after 30-day storage at 4 °C (data not shown).

Altogether, the results obtained from physicochemical characterization pointed out INC1 as the formulation with all the physicochemical properties within the acceptable range for ophthalmic use. The INC1 droplet size, zeta-potential, viscosity, osmolarity and surface tension resemble the values reported for NEs produced using Novasorb® technology (Lallemand et al., 2012). In addition, the INC1 formulation was found to be stable under all the experimental conditions tested.

3.3. Sterilization

Sterility is a basic requirement for ophthalmic NEs and filtration and/or autoclavation are usually used for sterilization of the final product. Clearly, elevated temperatures during the autoclavation, can seriously affect the final NE physicochemical characteristics. Autoclavation can cause hydrolysis of some lipids and lecithins, resulting in liberation of free fatty acids, which can compromise NE stability. Furthermore, it has already been reported that the autoclaving process can lead to destabilization of chitosan-coated lipid emulsions (Jumaa and Muller, 1999), which could be explained by temperature induced chitosan interchain crosslinking involving the amino groups (Lim et al., 1999). Indeed, autoclavation of the chitosan-coated NEs (NC1, NC2, INC1 and INC2) at 121 °C during 20 min resulted in meaningful changes in both physicochemical properties (increase in droplet size and PDI, reduction of zeta-potential, Fig. 4) and visual appearance (change in color and creaming). In contrast, NEs without chitosan (N and IN) showed satisfying stability after the autoclaving process regarding their droplet size, PDI and zeta-potential. However, filtration of chitosan-coated NEs through PES filters with 0.2 μm pore size did not affect any of the parameters tested (Fig. 4), as reported previously (Gue et al., 2016). Therefore, the final chitosan-coated NEs can be easily sterilized by aseptic filtration through a sterilizing membrane into a sterile suite (Floyd, 1999), without the need for aseptic preparation procedure.

3.4. In vitro ibuprofen release

In general, drug release from a NE involves partitioning of the drug from the oil droplets into the surfactant layer and then into the aqueous phase (Singh et al., 2017). While diffusing out from the oil, the drug comes in contact with the surrounding aqueous media and depending on its solubility and the volume of the aqueous media it can undergo nanoprecipitaion. Biorelevant methods for *in vitro* release testing of ophthalmic products are still in development (Jug et al., 2018). *In vitro* drug release from nano-sized ophthalmic delivery system is currently assessed using a variety of membrane diffusion techniques including simple dialysis methods, dialysis methods using modified Apparatus 1 or 2 as well as Franz diffusion cells (Jug et al., 2018). We chose a dialysis method using modified Apparatus 2, and since the concentration of ibuprofen present in the NE formulations exceeds ibuprofen water solubility (Hussain et al., 2018), a commercially available ibuprofen oral suspension (20 mg mL^{-1}; Neofen®, Belupo, Croatia), diluted with double-distilled water to the appropriate concentration, and ibuprofen oil (Miglyol® 812) solution were used as controls. The obtained *in vitro* release profiles are shown in Fig. 5. About 90% of ibuprofen was released from the NEs in 120 min. The t$_{50\%}$ of IN, INC1 and INC2 was 30, 35 and 41 min, respectively. Unsurprisingly, ibuprofen release was significantly faster from the NE formulations than from the ibuprofen suspension (t$_{50\%}$ = 68 min; f$_2$ < 45) and oil solution (t$_{50\%}$ = 94 min; f$_2$ < 30), due to the large total nanodroplet surface area available for drug diffusion in the NEs. Such a release profile could be beneficial regarding the limited drug residence at the ocular surface. The addition of chitosan to the NE formulation seemed to slightly slow down ibuprofen release, but the statistical significance was confirmed only

Table 6
Ibuprofen-loaded NEs characterized in terms of droplet size, PDI, zeta-potential, entrapment efficiency, pH, viscosity, osmolarity and surface tension.

Formulation	Droplet size (nm)	PDI	Zeta-potential (mV)	Entrapment efficiency (%)	pH	Viscosity (mPas)	Osmolarity (mOsm kg^{-1})	Surface tension (mN m^{-1})
IN	172.5 ± 0.4 (177.8 ± 1.1)	0.116 ± 0.017 (0.127 ± 0.013)	−15.6 ± 0.2 (-18.2 ± 3.5)	98.24 ± 0.10	4.42 ± 0.04 (5.83 ± 0.05)	1.1 ± 0 (1.1 ± 0.1)	271.0 ± 18.5 (275.5 ± 15.6)	38.9 ± 0.7 (42.4 ± 0.5)
INC1	175.1 ± 1.1 (183.9 ± 1.2)	0.127 ± 0.013 (0.114 ± 0.006)	24.6 ± 0.4 (18.0 ± 1.7)	98.73 ± 0.03	4.41 ± 0.03 (4.49 ± 0.01)	1.9 ± 0.1 (1.8 ± 0)	300.3 ± 1.0 (298.5 ± 1.3)	35.7 ± 0.3 (38.0 ± 0.7)
INC2	192.4 ± 28.9 (177.4 ± 2.6)	0.295 ± 0.120 (0.243 ± 0.024)	36.8 ± 2.0 (29.6 ± 1.5)	98.86 ± 0.01	4.42 ± 0.01 (4.39 ± 0.05)	4.1 ± 0.4 (4.0 ± 0.2)	291.5 ± 20.2 (316.5 ± 1.7)	34.5 ± 0.2 (39.4 ± 0.4)

Values are mean ± SD ($n \geq 3$); values in brackets refer to ibuprofen-free formulations.

between IN and INC2 formulations ($f_2 = 48$). This could be explained by localisation of chitosan molecules on the NE droplet surface, forming a certain barrier to ibuprofen release.

3.5. Chitosan-coated NE mucoadhesive properties

Mucoadhesive interactions between chitosan and mucin are complex and involve electrostatic attraction, hydrogen bonding, and hydrophobic effects (Sogias et al., 2008). The relative contributions of each physical interaction depend on the pH and ionic strength of the surrounding medium (Ding et al., 2019). Mucoadhesive properties of the chitosan-coated NEs were assessed by determining rheological behavior of mixtures of mucin dispersions in STF with the NE formulations (Hassan and Gallo, 1990). In this method, NEs were mixed with mucin dispersion in STF and a synergistic viscosity increase caused by interactions between NEs and mucin chains was recorded and calculated as η_b, according to Eq. (2). Interestingly, even anionic NE without chitosan (IN) showed mucoadhesive behavior, as the calculated η_b value was around 30 mPa s (Fig. 6). Chitosan-coated INC1 and INC2 formulations, on the other hand, showed significantly stronger mucoadhesion (INC1: P = 0.0210; INC2: P = 0.0184), having η_b of around 48 mPas, due to the well-known electrostatic interactions between positively charged chitosan molecules and negatively charged mucin chains (Sogias et al., 2008). However, there was no statistically significant difference between η_b of INC1 and INC2 formulations (P = 0.9927), indicating that higher chitosan concentration was not able to augment the effect of mucoadhesion of the NEs tested within this research.

3.6. Biocompatibility studies

3.6.1. In vitro corneal biocompatibility

An important aspect of topical ophthalmic formulation characterization is the investigation of formulation biocompatibility with the corneal epithelium. Although biocompatibility of chitosan is well-known, and it has been widely used in nanosystems investigated for topical ocular application, a concentration-dependent toxicity effect has been reported (de la Fuente et al., 2010; Diebold et al., 2007). Also, surfactants are able to non-specifically partition into the plasma membrane causing membrane fluidization, which is associated with the concentration-dependent increase in permeability but also toxicity, due to epithelial abrasion (Brayden et al., 2014). Even though surfactants have a long history of use in ophthalmic drug delivery and in this study surfactants normally present in the tear film as well as other ophthalmically acceptable formulation components were used, safety has to be evaluated *in vitro*. The most extensively characterized human-derived cell line used in corneal biocompatibility and transcorneal permeability studies is the immortalized human corneal epithelial cell line (HCE-T) (Juretic et al., 2017). The majority of *in vitro* biocompatibility screenings is currently undertaken using cells cultured in a two-dimensional (2D) environment (Fitzgerald et al., 2015). However, this does not accurately reflect the three-dimensional (3D) structure of corneal epithelium. The use of inadequate experimental tools can lead to wrong conclusions about formulation biocompatibility (Krtalic et al., 2018). Using 3D cell-based models it is possible to predict biocompatibility *in vivo* more closely than with the conventional 2D models because 3D models have more realistic representation of the tissue complexity, including drug, oxygen and nutrient gradients. Therefore, to test corneal epithelium biocompatibility we employed 3D HCE-T cell-based model. HCE-T corneal model viability was evaluated by colorimetric MTT assay after 30-min incubation with the NE samples and it was expressed as the percentage of mitochondrial dehydrogenase activity, using the cells treated with HBSS as the reference point (100% of mitochondrial dehydrogenase activity). As it can be seen from Fig. 7, the viability of the cells treated with ibuprofen suspension (IBU S) decreased to about 85%, which is significantly lower than the viability of
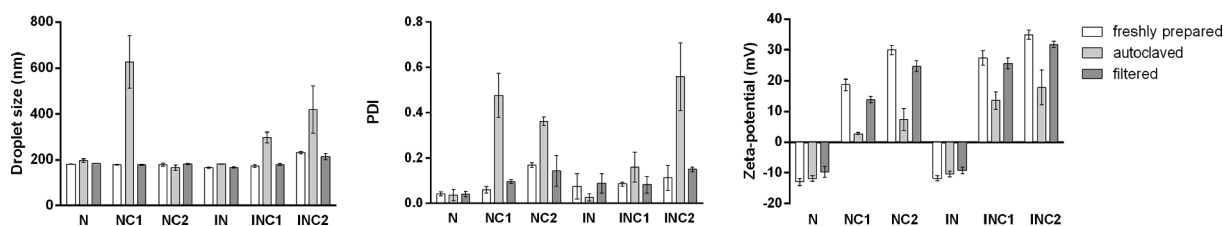
Fig. 4. Droplet size, PDI and zeta-potential of chitosan-coated NEs with 0.05% (*w/w*) chitosan and loaded with ibuprofen (INC1) or ibuprofen free (NC1), chitosan-coated NEs with 0.3% (*w/w*) chitosan and loaded with ibuprofen (INC2) or ibuprofen free (NC2), the uncoated control formulation loaded with ibuprofen (IN) or ibuprofen free (N) measured before and after autoclaving (121 °C/20 min) or filtration (PES; 0.2 μm). Data are expressed as mean ± SD ($n = 2$).
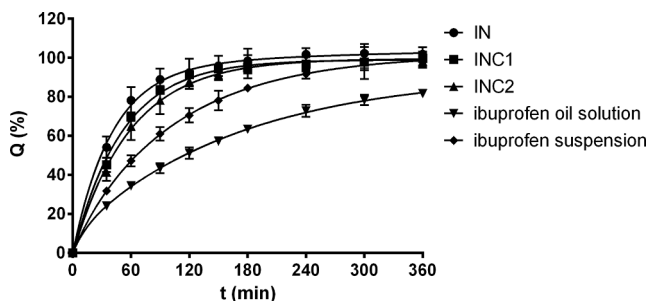

Fig. 5. *In vitro* release profiles of ibuprofen from chitosan-coated NEs with 0.05 (INC1) and 0.3 (INC2) % (*w/w*) chitosan, the uncoated control formulation (IN) and respective controls (ibuprofen oil solution and ibuprofen suspension) tested during 6 h (360 min) in phosphate buffer pH 7.4 at 34 °C. Data are expressed as mean ± SD (n = 3–6).
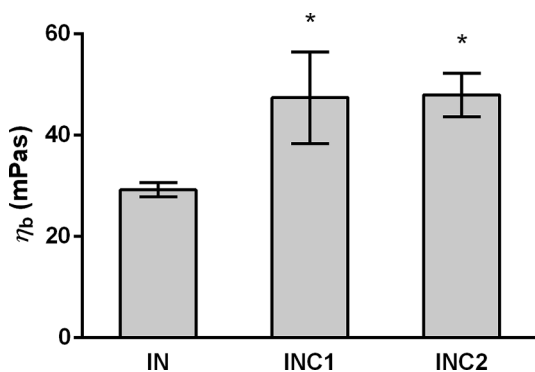
Fig. 6. Mucoadhesive properties of ibuprofen-loaded NEs determined rheologically after mixing with 20% (*w/w*) mucin dispersion in STF, expressed as the viscosity component due to bioadhesion (η_b). Data are expressed as mean ± SD ($n = 3$). *Differs from the uncoated IN formulation ($P < 0.05$).
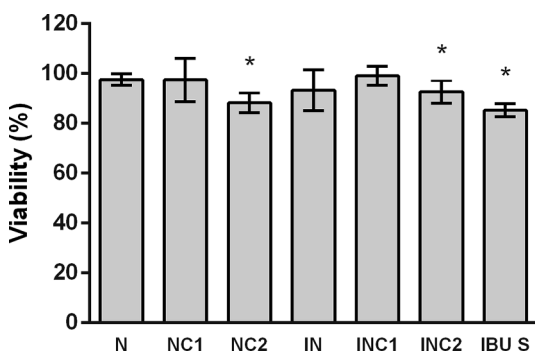

Fig. 7. *In vitro* 3D HCE-T model viability (%) determined by MTT assay after 30-min incubation with NE formulations (or ibuprofen suspension; IBU S) diluted 10 times (*V/V*) in HBSS pH 6.0. The cells incubated in HBSS pH 6.0 were used as control of 100% cell viability. Data are expressed as mean ± SD ($n = 6$). *Differs from the control ($P < 0.05$).

the control cells ($P = 0.0004$). Ibuprofen loaded formulations IN and INC1 (and the unloaded control formulations N and NC1), on the other hand, did not significantly affect viability of the cells. This can be explained by ibuprofen encapsulation into the oil nanodroplets, hindering its direct toxicity effect on the cells. However, the formulation INC2 and the control unloaded formulation NC2 showed significantly lower cell viability of 93% ($P = 0.0365$) and 88% ($P = 0.0004$), respectively. Taking everything into account, this small but significant viability decrease could be ascribed to higher concentration of chitosan (0.3%, *w/w*) in INC2 and NC2 formulations, which is in agreement with previously reported concentration-dependent toxicity of chitosan (Diebold et al., 2007).

3.6.2. Ex vivo corneal biocompatibility

To confirm the data obtained from the *in vitro* model, biocompatibility was also tested on the *ex vivo* model using freshly excised porcine corneas. The corneas were incubated with NEs during 5 and 15 min and the extent of corneal damage was evaluated visually using fluorescein solution and a cobalt blue lamp, since fluorescein staining is a well-known measure of corneal epithelial cell damage (Prinsen and Koeter, 1993). Photographs were taken after each incubation time point and they are shown in Fig. 8. While PBS (negative control) and ibuprofen suspension (IBU S; 0.2%, *w/V*) did not cause corneal epithelial damage, an intense staining was observed after incubation with 0.1 M NaOH solution and acetone (positive controls). Fluorescein staining was also observed on BAK treated corneas after 15-min incubation. BAK was applied as 0.025% (*w/V*) solution in PBS, since it is the highest concentration approved in the eye drops (FDA Database: Inactive ingredients). It can clearly be seen that IN and INC1 formulations did not cause any changes on the corneal surface since no fluorescein staining was detected, but the INC2 formulation caused a mild fluorescein staining after 15-min incubation, which is in agreement with the *in vitro* studies performed.

3.7. Conclusions

Herein we propose chitosan-coated NEs for improved NSAIDs delivery in the treatment of mild-to-moderate DED. The results of our study pointed out INC1 as the lead formulation, having physicochemical properties inside the appropriate range for ophthalmic application, adequate stability and the possibility to be easily sterilized after preparation. Also, the proposed formulation has significant mucoadhesive character, as confirmed by the *in vitro* studies, and excellent biocompatibility, which was tested on two models, namely 3D HCE-T cell-based model and *ex vivo* model using fresh porcine corneas. Development of formulations with prolonged residence at the ocular surface would enable reduction of the required NSAID dose providing better benefit-risk balance of future ophthalmic drug products. In addition, ibuprofen-free NC1 formulation could also be used as a drug-free vehicle (artificial tears) for symptomatic treatment of mild-to-moderate DED. However, further *in vivo* studies are necessary to confirm these conclusions.
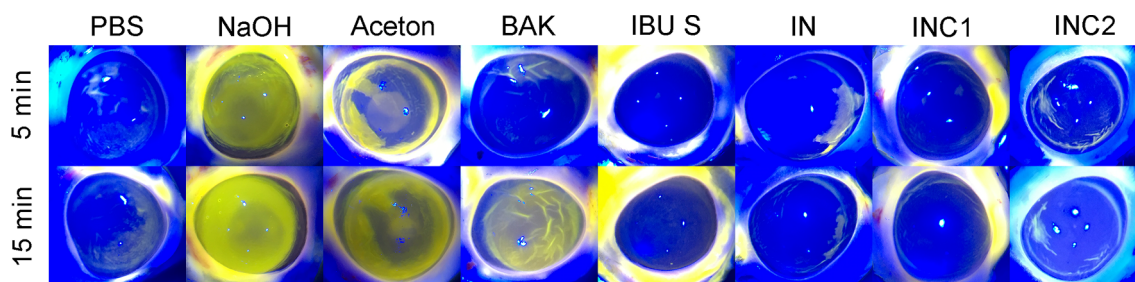
Fig. 8. Representative photographs of *ex vivo* model of porcine corneas captured after 5 and 15-minute treatment with ibuprofen-loaded NE*s* (IN, INC1 and INC2) or control samples (PBS pH 7.4, 0.1 M NaOH, aceton, 0.025%, *w/V* benzalkonium chloride solution (BAK) and 0.2%, *w/V* ibuprofen suspension (IBU S)) and subsequent fluorescein staining with the aid of a cobalt-blue lamp used to intensify the fluorescence signal ($n \geq 4$).

CRediT authorship contribution statement

Bisera Jurišić Dukovski: Conceptualization, Data curation, Formal analysis, Investigation, Methodology, Validation, Writing - original draft, Writing - review & editing. **Marina Juretić:** Formal analysis, Investigation, Methodology, Validation, Writing - review & editing. **Danka Bračko:** Methodology, Writing - review & editing. **Danijela Randjelović:** Data curation, Formal analysis. **Snežana Savić:** Writing - review & editing. **Mario Crespo Moral:** Methodology. **Yolanda Diebold:** Writing - review & editing. **Jelena Filipović-Grčić:** Funding acquisition, Writing - review & editing. **Ivan Pepić:** Methodology, Writing - review & editing. **Jasmina Lovrić:** Conceptualization, Data curation, Formal analysis, Funding acquisition, Investigation, Methodology, Project administration, Resources, Validation, Visualization, Writing - original draft, Writing - review & editing.

Declaration of Competing Interest

The authors declare that they have no known competing financial interests or personal relationships that could have appeared to influence the work reported in this paper.

Appendix A. Supplementary material

Supplementary data to this article can be found online at https://doi.org/10.1016/j.ijpharm.2019.118979.

References

Acar, D., Molina-Martinez, I.T., Gomez-Ballesteros, M., Guzman-Navarro, M., Benitez-Del-Castillo, J.M., Herrero-Vanrell, R., 2018. Novel liposome-based and in situ gelling artificial tear formulation for dry eye disease treatment. Cont. Lens. Anterior. Eye 41, 93–96.

Baudouin, C., Aragona, P., Messmer, E.M., Tomlinson, A., Calonge, M., Boboridis, K.G., Akova, Y.A., Geerling, G., Labetoulle, M., Rolando, M., 2013. Role of hyperosmolarity in the pathogenesis and management of dry eye disease: proceedings of the OCEAN group meeting. Ocul. Surf. 11, 246–258.

Baydoun, L., Duvel, A., Daniels, R., Drust, A., Goldhagen, T., Schwan, I., Zeidler, C.,

Muller-Goymann, C.C., 2004. Comparison of different ibuprofen-amino acid compounds with respect to emulsifying and cytotoxic properties. Int. J. Pharm. 274, 157–165.

Benelli, U., 2011. Systane lubricant eye drops in the management of ocular dryness. Clin. Ophthalmol. 5, 783–790.

Brayden, D.J., Gleeson, J., Walsh, E.G., 2014. A head-to-head multi-parametric high content analysis of a series of medium chain fatty acid intestinal permeation enhancers in Caco-2 cells. Eur. J. Pharm. Biopharm. 88, 830–839.

Bron, A.J., de Paiva, C.S., Chauhan, S.K., Bonini, S., Gabison, E.E., Jain, S., Knop, E., Markoulli, M., Ogawa, Y., Perez, V., Uchino, Y., Yokoi, N., Zoukhri, D., Sullivan, D.A., 2017. TFOS DEWS II Pathophysiology report. Ocul. Surf. 15, 438–510.

Craig, J.P., Nichols, K.K., Akpek, E.K., Caffery, B., Dua, H.S., Joo, C.K., Liu, Z., Nelson, J.D., Nichols, J.J., Tsubota, K., Stapleton, F., 2017. TFOS DEWS II definition and classification report. Ocul. Surf. 15, 276–283.

Daull, P., Lallemand, F., Garrigue, J.S., 2014. Benefits of cetalkonium chloride cationic oil-in-water nanoemulsions for topical ophthalmic drug delivery. J. Pharm. Pharmacol. 66, 531–541.

de la Fuente, M., Ravina, M., Paolicelli, P., Sanchez, A., Seijo, B., Alonso, M.J., 2010. Chitosan-based nanostructures: a delivery platform for ocular therapeutics. Adv. Drug Deliv. Rev. 62, 100–117.

Dean, A.W., Glasgow, B.J., 2012. Mass spectrometric identification of phospholipids in human tears and tear lipocalin. Invest. Ophthalmol. Vis. Sci. 53, 1773–1782.

Diaz, D.A., Colgan, S.T., Langer, C.S., Bandi, N.T., Likar, M.D., Van Alstine, L., 2016. Dissolution similarity requirements: how similar or dissimilar are the global regulatory expectations? AAPS J. 18, 15–22.

Diebold, Y., Jarrin, M., Saez, V., Carvalho, E.L., Orea, M., Calonge, M., Seijo, B., Alonso, M.J., 2007. Ocular drug delivery by liposome-chitosan nanoparticle complexes (LCS-NP). Biomaterials 28, 1553–1564.

Ding, L., Huang, Y., Cai, X., Wang, S., 2019. Impact of pH, ionic strength and chitosan charge density on chitosan/casein complexation and phase behavior. Carbohydr. Polym. 208, 133–141.

Fialho, S.L., da Silva-Cunha, A., 2004. New vehicle based on a microemulsion for topical ocular administration of dexamethasone. Clin. Exp. Ophthalmol. 32, 626–632.

Fitzgerald, K.A., Malhotra, M., Curtin, C.M., FJ, O.B., CM, O.D., 2015. Life in 3D is never flat: 3D models to optimise drug delivery. J. Control Release 215, 39–54.

Floyd, A.G., 1999. Top ten considerations in the development of parenteral emulsions. Pharm. Sci. Technol. Today 4, 134–143.

Gan, L., Wang, J., Jiang, M., Bartlett, H., Ouyang, D., Eperjesi, F., Liu, J., Gan, Y., 2013. Recent advances in topical ophthalmic drug delivery with lipid-based nanocarriers. Drug Discov. Today 18, 290–297.

Gue, E., Since, M., Ropars, S., Herbinet, R., Le Pluart, L., Malzert-Freon, A., 2016. Evaluation of the versatile character of a nanoemulsion formulation. Int. J. Pharm. 498, 49–65.

Hafner, A., Lovric, J., Voinovich, D., Filipovic-Grcic, J., 2009. Melatonin-loaded lecithin/chitosan nanoparticles: physicochemical characterisation and permeability through Caco-2 cell monolayers. Int. J. Pharm. 381, 205–213.

Hassan, E.E., Gallo, J.M., 1990. A simple rheological method for the in vitro assessment of mucin-polymer bioadhesive bond strength. Pharm. Res. 7, 491–495.

Hotujac Grgurevic, M., Juretic, M., Hafner, A., Lovric, J., Pepic, I., 2017. Tear fluid-eye drops compatibility assessment using surface tension. Drug Dev. Ind. Pharm. 43, 275–282.

Hussain, A., Smith, G., Khan, K.A., Bukhari, N.I., Pedge, N.I., Ermolina, I., 2018. Solubility and dissolution rate enhancement of ibuprofen by co-milling with polymeric excipients. Eur. J. Pharm. Sci. 123, 395–403.

Jones, L., Downie, L.E., Korb, D., Benitez-Del-Castillo, J.M., Dana, R., Deng, S.X., Dong, P.N., Geerling, G., Hida, R.Y., Liu, Y., Seo, K.Y., Tauber, J., Wakamatsu, T.H., Xu, J., Wolffsohn, J.S., Craig, J.P., 2017. TFOS DEWS II management and therapy report. Ocul. Surf. 15, 575–628.

Jug, M., Hafner, A., Lovric, J., Kregar, M.L., Pepic, I., Vanic, Z., Cetina-Cizmek, B., Filipovic-Grcic, J., 2018. An overview of in vitro dissolution/release methods for novel mucosal drug delivery systems. J. Pharm. Biomed. Anal. 147, 350–366.

Jumaa, M., Muller, B.W., 1999. Physicochemical properties of chitosan-lipid emulsions and their stability during the autoclaving process. Int. J. Pharm. 183, 175–184.

Juretic, M., Jurisic Dukovski, B., Krtalic, I., Reichl, S., Cetina-Cizmek, B., Filipovic-Grcic, J., Lovric, J., Pepic, I., 2017. HCE-T cell-based permeability model: a well-maintained or a highly variable barrier phenotype? Eur. J. Pharm. Sci. 104, 23–30.

Khurana, A.K., Chaudhary, R., Ahluwalia, B.K., Gupta, S., 1991. Tear film profile in dry

eye. Acta Ophthalmol. (Copenh) 69, 79–86.

Kinnunen, K., Kauppinen, A., Piippo, N., Koistinen, A., Toropainen, E., Kaarniranta, K., 2014. Cationorm shows good tolerability on human HCE-2 corneal epithelial cell cultures. Exp. Eye Res. 120, 82–89.

Klang, V., Valenta, C., 2011. Lecithin-based nanoemulsions. J. Drug Deliv. Sci. Technol. 21.

Krtalic, I., Radosevic, S., Hafner, A., Grassi, M., Nenadic, M., Cetina-Cizmek, B., Filipovic-Grcic, J., Pepic, I., Lovric, J., 2018. D-Optimal design in the development of rheologically improved in situ forming ophthalmic gel. J. Pharm. Sci. 107, 1562–1571.

Lallemand, F., Daull, P., Benita, S., Buggage, R., Garrigue, J.S., 2012. Successfully improving ocular drug delivery using the cationic nanoemulsion, novasorb. J. Drug Deliv. 2012, 604204.

Lallemand, F., Schmitt, M., Bourges, J.L., Gurny, R., Benita, S., Garrigue, J.S., 2017. Cyclosporine A delivery to the eye: a comprehensive review of academic and industrial efforts. Eur. J. Pharm. Biopharm. 117, 14–28.

Lalu, L., Tambe, V., Pradhan, D., Nayak, K., Bagchi, S., Maheshwari, R., Kalia, K., Tekade, R.K., 2017. Novel nanosystems for the treatment of ocular inflammation: current paradigms and future research directions. J. Control. Release 268, 19–39.

Lang, J.C., Roehrs, R.E., Jani, R., 2005. Ophthalmic preparations. In: Troy, D.B., Beringer, P. (Eds.), Remington: The Science and Practice of Pharmacy, 21st ed. LippincottWilliamsWilkins, Philadelphia, PA, USA, pp. 861–862.

Li, J., Hwang, I.-C., Chen, X., Park, H.J., 2016. Effects of chitosan coating on curcumin loaded nano-emulsion: study on stability and in vitro digestibility. Food Hydrocolloids 60, 138–147.

Lim, L.Y., Khor, E., Ling, C.E., 1999. Effects of dry heat and saturated steam on the physical properties of chitosan. J. Biomed. Mater. Res. 48, 111–116.

Ludwig, A., Reimann, H., 2015. Eye. In: Bouwman-Boer, Y., Fenton-May, V., Le Brun, P. (Eds.), Practical Pharmaceutics. KNMP and Springer International, Ny, pp. 163–188.

McCulley, J.P., Shine, W., 1997. A compositional based model for the tear film lipid layer. Trans. Am. Ophthalmol. Soc. 95, 79–88 discussion 88–93.

Meleson, K., Graves, S., Mason, T.G., 2004. Formation of concentrated nanoemulsions by extreme shear. Soft Mater. 2, 109–123.

Mun, S., Decker, E.A., McClements, D.J., 2006. Effect of molecular weight and degree of deacetylation of chitosan on the formation of oil-in-water emulsions stabilized by surfactant-chitosan membranes. J. Colloid Interface Sci. 296, 581–590.

Nagyova, B., Tiffany, J.M., 1999. Components responsible for the surface tension of human tears. Curr. Eye Res. 19, 4–11.

Nguyen, S., Hisiger, S., Jolicoeur, M., Winnik, F.M., Buschmann, M.D., 2009. Fractionation and characterization of chitosan by analytical SEC and 1H NMR after semi-preparative SEC. Carbohydr. Polym. 75, 636–645.

Norn, M.S., 1988. Tear fluid pH in normals, contact lens wearers, and pathological cases. Acta Ophthalmol. (Copenh) 66, 485–489.

Pandit, J.C., Nagyova, B., Bron, A.J., Tiffany, J.M., 1999. Physical properties of stimulated and unstimulated tears. Exp. Eye Res. 68, 247–253.

Pauly, A., Meloni, M., Brignole-Baudouin, F., Warnet, J.M., Baudouin, C., 2009. Multiple endpoint analysis of the 3D-reconstituted corneal epithelium after treatment with benzalkonium chloride: early detection of toxic damage. Invest. Ophthalmol. Vis. Sci. 50, 1644–1652.

Payet, L., Terentjev, E.M., 2008. Emulsification and stabilization mechanisms of o/w emulsions in the presence of chitosan. Langmuir 24, 12247–12252.

Prinsen, M.K., Koeter, H.B., 1993. Justification of the enucleated eye test with eyes of slaughterhouse animals as an alternative to the Draize eye irritation test with rabbits. Food Chem. Toxicol. 31, 69–76.

Qu, H., Wang, J., Wu, Y., Zheng, J., Krishnaiah, Y.S.R., Absar, M., Choi, S., Ashraf, M., Cruz, C.N., Xu, X., 2018. Asymmetric flow field flow fractionation for the characterization of globule size distribution in complex formulations: a cyclosporine ophthalmic emulsion case. Int. J. Pharm. 538, 215–222.

Rai, V.K., Mishra, N., Yadav, K.S., Yadav, N.P., 2018. Nanoemulsion as pharmaceutical carrier for dermal and transdermal drug delivery: formulation development, stability issues, basic considerations and applications. J. Control. Release 270, 203–225.

Rao, C.S., Schoenwald, R.D., Barfknecht, C.F., Laban, S.L., 1992. Biopharmaceutical evaluation of ibufenac, ibuprofen, and their hydroxyethoxy analogs in the rabbit eye. J. Pharmacokinet. Biopharm. 20, 357–388.

Rinaudo, M., 2016. Chitin and chitosan: properties and applications. Prog. Polym. Sc. 31, 603–632.

Saville, J.T., Zhao, Z., Willcox, M.D., Ariyavidana, M.A., Blanksby, S.J., Mitchell, T.W., 2011. Identification of phospholipids in human meibum by nano-electrospray ionisation tandem mass spectrometry. Exp. Eye Res. 92, 238–240.

Shafiq, S., Shakeel, F., Talegaonkar, S., Ahmad, F.J., Khar, R.K., Ali, M., 2007. Development and bioavailability assessment of ramipril nanoemulsion formulation. Eur. J. Pharm. Biopharm. 66, 227–243.

Shine, W.E., McCulley, J.P., 1998. Keratoconjunctivitis sicca associated with meibomian secretion polar lipid abnormality. Arch. Ophthalmol. 116, 849–852.

Simmons, P.A., Vehige, J.G., 2007. Clinical performance of a mid-viscosity artificial tear for dry eye treatment. Cornea 26, 294–302.

Singh, Y., Meher, J.G., Raval, K., Khan, F.A., Chaurasia, M., Jain, N.K., Chourasia, M.K., 2017. Nanoemulsion: concepts, development and applications in drug delivery. J. Control. Release 252, 28–49.

Sogias, I.A., Williams, A.C., Khutoryanskiy, V.V., 2008. Why is chitosan mucoadhesive? Biomacromolecules 9, 1837–1842.

Stevenson, D., Tauber, J., Reis, B.L., 2000. Efficacy and safety of cyclosporin A ophthalmic emulsion in the treatment of moderate-to-severe dry eye disease: a dose-ranging, randomized trial. The Cyclosporin A Phase 2 Study Group. Ophthalmology 107, 967–974.

Subrizi, A., Del Amo, E.M., Korzhikov-Vlakh, V., Tennikova, T., Ruponen, M., Urtti, A., 2019. Design principles of ocular drug delivery systems: importance of drug payload, release rate, and material properties. Drug Discov. Today.

Tamilvanan, S., Benita, S., 2004. The potential of lipid emulsion for ocular delivery of lipophilic drugs. Eur. J. Pharm. Biopharm. 58, 357–368.

Teixeira, H.F., Bruxel, F., Fraga, M., Schuh, R.S., Zorzi, G.K., Matte, U., Fattal, E., 2017. Cationic nanoemulsions as nucleic acids delivery systems. Int. J. Pharm. 534, 356–367.

Tiffany, J.M., 1991. The viscosity of human tears. Int. Ophthalmol. 15, 371–376.

Trotta, M., Pattarino, F., Ignoni, T., 2002. Stability of drug-carrier emulsions containing phosphatidylcholine mixtures. Eur. J. Pharm. Biopharm. 53, 203–208.

Uluata, S., Decker, E.A., McClements, D.J., 2016. Optimization of nanoemulsion fabrication using microfluidization: role of surfactant concentration on formation and stability. Food Biophys. 11, 52–59.

Walenga, R.L., Babiskin, A.H., Zhang, X., Absar, M., Zhao, L., Lionberger, R.A., 2019. Impact of vehicle physicochemical properties on modeling-based predictions of cyclosporine ophthalmic emulsion bioavailability and tear film breakup time. J. Pharm. Sci. 108, 620–629.

Willcox, M.D.P., Argueso, P., Georgiev, G.A., Holopainen, J.M., Laurie, G.W., Millar, T.J., Papas, E.B., Rolland, J.P., Schmidt, T.A., Stahl, U., Suarez, T., Subbaraman, L.N., Ucakhan, O.O., Jones, L., 2017. TFOS DEWS II tear film report. Ocul. Surf. 15, 366–403.

Yamada, M., Kawai, M., Mochizuki, H., Hata, Y., Mashima, Y., 1998. Fluorophotometric measurement of the buffering action of human tears in vivo. Curr. Eye Res. 17, 1005–1009.